

Discovery of a very Lyman- α -luminous quasar at $z=6.62$

Ekaterina Koptelova^{1,*}, Chorong-Yuan Hwang^{1,*}, Po-Chieh Yu^{1,+}, Wen-Ping Chen^{1,+}, and Jhen-Kuei Guo^{1,+}

¹National Central University, Graduate Institute of Astronomy, Taoyuan City, 32001, Taiwan

*koptelova@astro.ncu.edu.tw

*hwangcy@astro.ncu.edu.tw

+these authors contributed equally to this work

ABSTRACT

Distant luminous quasars provide important information on the growth of the first supermassive black holes, their host galaxies and the epoch of reionization. The identification of quasars is usually performed through detection of their Lyman- α line redshifted to $\gtrsim 0.9$ microns at $z > 6.5$. Here, we report the discovery of a very Lyman- α luminous quasar, PSO J006.1240+39.2219 at redshift $z=6.618$, selected based on its red colour and multi-epoch detection of the Lyman- α emission in a single near-infrared band. The Lyman- α line luminosity of PSO J006.1240+39.2219 is unusually high and estimated to be 0.8×10^{12} Solar luminosities (about 3% of the total quasar luminosity). The Lyman- α emission of PSO J006.1240+39.2219 shows fast variability on timescales of days in the quasar rest frame, which has never been detected in any of the known high-redshift quasars. The high luminosity of the Lyman- α line, its narrow width and fast variability resemble properties of local Narrow-Line Seyfert 1 galaxies which suggests that the quasar is likely at the active phase of the black hole growth accreting close or even beyond the Eddington limit.

Introduction

High-redshift quasars provide important constraints on theories of structure formation and properties of the intergalactic medium (IGM) at early cosmic epochs. The most distant of them are seen at redshifts $z > 6.5$ (when the Universe was less than 6% of its present age), before the end of reionization¹. There are only seven quasars found at $z > 6.5$. Four were discovered in near-infrared surveys^{2,3}. Three new quasars⁴ were discovered recently from the 3π Panoramic Survey Telescope and Rapid Response System^{5,6} (Pan-STARRS1 or PS1) sensitive up to the near-infrared y_{PS1} band ($\lambda_{\text{eff}}=0.96\mu\text{m}$). These highest-redshift quasars host the most massive supermassive black holes

(SMBHs) with masses 10^9 - $10^{10} M_{\odot}$ (where M_{\odot} is the solar mass) accreting close to the Eddington luminosity^{2,7,8}.

We used the PS1 data to search for new quasars at $z > 6.5$ among extremely red sources with colours $z_{PS1} - y_{PS1} > 2$ mag and multiple detections at several different epochs (see 'Quasar candidate selection' in the Methods). In our follow-up observations of these sources on November 2, 2015 we discovered a new high-redshift quasar, PSO J006.1240+39.2219, at $z=6.618$ (see 'Spectroscopic follow-up' and 'Redshift measurements' in the Methods).

Results

The discovery spectrum of PSO J006.1240+39.2219 shows an unusually strong, compared to the continuum and, at the same time, narrow Lyman- α ($Ly\alpha$) emission line with a line width of $1300 \pm 90 \text{ km s}^{-1}$ (see Fig. 1). This line width is smaller than the typical width of the emission lines produced in the Broad Line Region (BLR) of quasars. For comparison, we estimated the $Ly\alpha$ line width of the quasars known at $z > 6.5$ to be between 2000 and 3800 km s^{-1} . The observed metal lines of PSO J006.1240+39.2219 (NV, OI+SiII and CII) do not exhibit the unusual strength as its $Ly\alpha$ line. As seen in Fig. 1, the peak flux ratio of the $Ly\alpha$ and NV lines of PSO J006.1240+39.2219 is more than twice larger than that observed in high-redshift quasars with strong $Ly\alpha$ emission⁹. The small width of the $Ly\alpha$ line of PSO J006.1240+39.2219 is difficult to explain as due to particularly strong absorption by neutral hydrogen (HI). The absorption features on the blue side of the line have a minor impact on its strength and shape (the core of the line is rather symmetric relative to the redshifted line wavelength). This might imply that the $Ly\alpha$ line of PSO J006.1240+39.2219 is dominated by a narrow-line component and its profile is intrinsically narrow. In the local Universe, narrow high-ionization, broad emission lines are also observed in Narrow-Line Seyfert 1 (NLS1) galaxies. As demonstrated in Fig. 1, the $Ly\alpha$ line of the NLS1s is much stronger than in broad-line quasars¹⁰. The NLS1 galaxies have smaller black holes of 10^6 - $10^8 M_{\odot}$ resulting in the narrow width of the BLR lines. Most of the NLS1s accrete at the super-Eddington limit¹¹⁻¹³.

From power-law fit $F_{\lambda} \sim \lambda^{\alpha}$ to the continuum of PSO J006.1240+39.2219 between 9500-9900 and 10000-10150 \AA , we estimated a spectral slope of $\alpha = -1.10 \pm 0.48$. By extrapolating the power law to $1450 \times (1+z) \text{\AA}$, we measured the absolute magnitude of the quasar at rest-frame wavelength 1450 \AA to be $M_{1450} = -26.1 \pm 0.4$, where the error includes the uncertainty in the spectral slope and redshift. Applying a bolometric correction factor of 4.4 to the ultraviolet (UV) luminosity¹⁴, we estimated a total quasar luminosity of $2.8 \times 10^{13} L_{\odot}$ (where L_{\odot} is the solar luminosity). The relation between black hole mass and bolometric luminosity for the known $z \sim 6$ quasars follows well the expected relation for accretion at the Eddington limit¹⁵. If PSO J006.1240+39.2219 accretes at the Eddington limit, its luminosity implies a black hole mass of 10^8 - $10^9 M_{\odot}$ ^{7,15}. Given the relation between mass of black holes and square of the width of broad emission lines¹⁶, the narrow $Ly\alpha$ line of PSO J006.1240+39.2219

implies up to an order of a magnitude smaller black hole mass than expected from the quasar luminosity, and the super-Eddington accretion rate^{7,15}.

From the spectrum of PSO J006.1240+39.2219 with the subtracted continuum we measured its Ly α line luminosity to be $0.8 \times 10^{12} L_{\odot}$, which is about 3% of the total luminosity of the quasar. We compared the luminosity of the Ly α line of PSO J006.1240+39.2219 with that of the other quasars discovered at $z > 6.5$. As shown in Fig. 2, the Ly α luminosity of PSO J006.1240+39.2219 is larger than the Ly α luminosity of the $z > 6.5$ quasars by more than a factor of two. It is also more than ten times larger than the Ly α luminosity of the most luminous Lyman Alpha Emitting galaxies (LAEs) seen during the epoch of reionization¹⁷. The relative contribution of the Ly α line into the total quasar luminosity is somewhat uncertain as due to the uncertainty in the continuum fit. However, we calculated that for power-law slopes between -0.5 and -2.5, the Ly α emission always dominates the UV continuum and contributes 2–4% into the bolometric luminosity of the quasar. In the other $z > 6.5$ quasars this contribution is only 0.1–0.5% (see Fig. 3). The rest-frame equivalent width (EW) of the Ly α line of PSO J006.1240+39.2219 is also large. Similar to the previous studies, we estimated the EW of the quasar by integrating the line flux above the continuum within $1160 < \lambda_{\text{rest}} < 1290 \text{ \AA}$, which includes the Ly α and NV lines. The measured EW of PSO J006.1240+39.2219 is equal to 182 \AA and corresponds to the high end of the equivalent width distribution of the known $z > 5.6$ quasars with the peak at $\text{EW} \approx 35 \text{ \AA}$ ⁹. Many of the $z > 5.6$ quasars have absolute magnitudes brighter than that of PSO J006.1240+39.2219, but only small fraction of them exhibit strong Ly α emission lines (Their composite spectrum is shown in Fig. 1). The typical EW of these quasars is $\sim 140 \text{ \AA}$ ⁹. The EWs of the known $z > 6.5$ quasars are smaller than 35 \AA (except for PSO J338+29 with $\text{EW} \simeq 70 \text{ \AA}$ ⁴), i.e., corresponds to the lower end of the EW distribution of the high-redshift quasars, which can be explained by stronger HI absorption at $z > 6.5$. The large EW of PSO J006.1240+39.2219 compared to these quasars implies weaker nearby intergalactic HI absorption.

The multi-epoch photometry of PSO J006.1240+39.2219 shows the change of the quasar brightness. From the PS1 images taken between June 2010 and July 2013, we measured the y_{PS1} -band brightness of the quasar at different epochs. The resulting quasar light curve is shown in Fig. 4. The brightness of the quasar at the time of our spectroscopic observations is also presented. From the quasar light curve we find that the quasar is variable on rest-frame timescales of days and months, with an amplitude exceeding its multi-epoch mean brightness by more than 2.5σ . The overall peak-to-peak amplitude of the observed variations is ~ 0.7 mag. Between 2010 and 2011, the quasar became brighter by about 0.24 mag within 50 days in the quasar rest frame. In 2013, PSO J006.1240+39.2219 changed its brightness from 20.15 ± 0.09 to 19.66 ± 0.07 mag over a period of ~ 2 days in the quasar rest frame. These high-amplitude variations are larger than brightness changes of 0.1–0.2 mag expected from

the UV/optical structure function¹⁸ and damped random walk model¹⁹ of quasar variability on similar timescales. However, we note, that the Ly α line is ionized by the extreme UV and soft X-ray radiation which can be highly variable. For instance, the soft X-ray flux of NLS1s can change by a factor of ten on timescales of days^{20,21}. The variation in Ly α emission can occur almost simultaneously with the variation of the ionizing flux on short timescales limited by hydrogen recombination time $\tau_{\text{rec}} = (n_e \alpha_B)^{-1} \approx 40(n_e/10^{11} \text{cm}^{-3})^{-1}$ s (where the typical electron density of the broad-line emitting gas is $n_e \gtrsim 10^8 \text{cm}^{-3}$ ²²) and the size of the Ly α emitting region^{23,24}.

The y_{PS1} band measures the total flux from the Ly α line and nearby UV continuum. Therefore, observed variability of PSO J006.1240+39.2219 can be caused both by the line and continuum variations. However, the continuum brightness, corresponding to the y_{PS1} -band multi-epoch mean quasar flux, is $\gtrsim 21$ mag, which is below the detection limit for single exposures in the 3π PS1 survey ($m_{y_{\text{PS1}}}^{\text{lim}} = 20.12$ mag)²⁵. The relative flux contribution of the Ly α line into the y_{PS1} -band total flux of the quasar is more than 70%. Therefore, the observed flux mostly comes from the Ly α line of PSO J006.1240+39.2219. The rapid y_{PS1} -band variations of the quasar provide the evidence of variable Ly α emission which responds fast to the variations of the extreme UV and soft X-ray flux and, therefore, originates close to the central engine²⁶. The small size of the Ly α emitting region, as expected from variability of the quasar, suggests a rather small mass of the central black hole¹⁶.

Discussion

We reported the discovery of the Ly α -luminous narrow-line quasar, PSO J006.1240+39.2219, with the first evidence of broad-band quasar variability at high redshift. We find a similarity between the properties of PSO J006.1240+39.2219 and the NLS1 galaxies. The NLS1s exhibit rapid UV variability and narrow broad lines, as a result of the smaller black hole masses, an order of a magnitude smaller than the black hole masses of the broad-line quasars of the same luminosities. Similar to the NLS1s, the strong narrow Ly α line of PSO J006.1240+39.2219 without a prominent broad-line component and its short-term variability provide the evidence of the smaller black hole mass of this quasar than that expected from the luminosity - black hole mass relation.

The high luminosity of the Ly α line of PSO J006.1240+39.2219 implies that the extreme UV and soft X-ray component of the quasar continuum is strong and sustains its Ly α emission at a very high level^{27,28}. We estimate the luminosity of this high-energy continuum to be $L_{\text{ion}} = 1.8 L(\text{Ly}\alpha)/f_{\text{esc}}^{\text{Ly}\alpha} \approx 5 \times 10^{12} L_{\odot}$ ²⁹, where we assume that the average energy of ionizing photons is 13.6eV and escape fraction of the Ly α photons is $f_{\text{esc}}^{\text{Ly}\alpha} \approx 0.3$. The adopted escape fraction represents the volume-averaged value that is found to evolve approximately as power law $f_{\text{esc}}^{\text{Ly}\alpha} \propto (1+z)^{2.57}$ between redshift 0 and 6³⁰. We note, that the volume-averaged escape fraction includes effects of absorption by the IGM that might lead to the smaller values of $f_{\text{esc}}^{\text{Ly}\alpha}$ at $z > 6$. In spite of the uncertainty in $f_{\text{esc}}^{\text{Ly}\alpha}$, being

the most luminous Ly α emitter, PSO J006.1240+39.2219 is the powerful source of ionizing radiation which likely has an important contribution into ionization of the IGM surrounding the quasar. From the observed spectrum we measure the size of the quasar ionized HII region scaled to $M_{1450} = -27$ to be $R_{\text{NZ}}=4\pm 1$ Mpc, which is slightly larger than a near zone of 2.5-3.5 Mpc expected from the empirical relation between R_{NZ} and redshift³¹ (see 'The near-zone size' in the Methods).

The observed y_{PS1} -band brightness variations of PSO J006.1240+39.2219 are likely due to variability of its Ly α emission as it substantially dominates the y_{PS1} -band flux of the quasar. The size of the Ly α emitting region of PSO J006.1240+39.2219 inferred from the timescale of the Ly α rapid variations is about 2 light days. This is similar but slightly smaller than the BLR regions of the local NLS1 galaxies^{24,32,33}. From the observations of reverberation time lags between the UV/X-ray continuum and Ly α line (and also between the UV/X-ray continuum and Balmer lines), the typical size of the Ly α emitting region of the NLS1s is estimated to be 3-10 light days. For comparison, the time lags (and correspondingly the BLR sizes) in broad-line quasars are ≥ 1 month^{34,35}. We caution that if the UV continuum of PSO J006.1240+39.2219 is highly variable (e.g., changing by about 1 mag on short timescales) its variability imposed on the variations of the Ly α flux would lead to underestimation of the size of the Ly α emitting region inferred from the observed short-term variations.

From the similarity of PSO J006.1240+39.2219 with the NLS1 galaxies we infer that this quasar is young, at the early phase of its black hole and bulge formation. These Ly α -line luminous young quasars seen at early cosmic epochs might be capable of ionizing large volumes of gas and might play a significant role in cosmic reionization.

Methods

Quasar candidate selection. We searched for z_{PS1} -band dropouts in the first and second internal data releases of the PS1 survey (PV1 and PV2) using the i_{PS1} -, z_{PS1} - and y_{PS1} -band photometric catalogues. First, from the y_{PS1} -band catalogue we selected point sources assuming that the difference between their point spread function (PSF) and aperture magnitudes is less than 0.3 mag, and the chi-square of the PSF fit is $\chi_{\text{red}}^2 < 1.5$. From the resulting sample we selected the z_{PS1} -band dropout quasar candidates using the following criteria: $z_{\text{PS1}} - y_{\text{PS1}} > 2$, $\sigma_{y_{\text{PS1}}} < 0.1$ mag (where $\sigma_{y_{\text{PS1}}}$ is the y_{PS1} -band photometric error), $i_{\text{PS1}} > 24$ and $z_{\text{PS1}} > 24$ mag. These criteria are similar to those adopted in the previous searches of high-redshift quasars from PS1⁴. Unlike the previous works, we additionally checked for multi-epoch detections of our z_{PS1} -band dropout candidates in the y_{PS1} -band. The PS1 survey conducted repeated scans of the sky and provided multi-epoch photometry for detected sources in all PS1 bands. The z_{PS1} -dropout candidates detected at least at two different epochs were considered by us as reliable. In this way we excluded short-lived transients and other possible artifacts from our colour-selected sample. The strongest of the

multi-epoch candidates had photometric measurements at five different epochs while no detection in the z_{PS1} band. This candidate is the high-redshift quasar presented in this work. The selected high-redshift quasar candidates were also checked for the counterparts in the Wide-Field Infrared Survey Explorer all-sky source catalogue³⁶ (AllWISE) within a match radius of 3 arcsec. However, none of them was detected in the WISE bands. Using this result, we place upper limits on their WISE W1 and W2 magnitudes to be $W1 > 19.7$ and $W2 > 19.3$ mag (i.e., fainter than the WISE W1 and W2 limiting magnitudes).

Spectroscopic follow-up. We performed simultaneous photometric and spectroscopic observations of twelve $z > 6.5$ quasar candidates with the Subaru Faint Object Camera And Spectrograph³⁷ (FOCAS) of the 8.2-m Subaru telescope. The observations were carried out on November 2, 2015. We used FOCAS long-slit mode, VPH900 grating and the SO58 order cut filter, giving us a wavelength coverage of 7500-10450Å and a dispersion of 0.74 Å pixel⁻¹. The slit was 0.8 arcsec wide resulting in a spectroscopic resolution of $R \sim 1500$. The seeing during the observations varied between 0.26-0.48 arcsec. Prior to spectroscopy we took acquisition images of the candidates in the FOCAS Y band. The spectra were taken only for three candidates, two of which were reliably detected during acquisition. Out of these three targets, only one had the blue-end cutoff typical for high-redshift sources. We took five 1000s through-slit exposures of this target which was identified as a quasar based on its spectrum. The stacked spectrum of the quasar and its uncertainty were calculated using median combine of the individual exposures. The quasar spectrum was absolute flux calibrated using the spectrophotometric standard star BD+28d4211 observed on the same night.

Redshift measurements. To estimate the redshift of the quasar, we measured the redshifted positions of the NV, OI+SiIII and CII emission lines at $\lambda_{\text{rest}} = 1239.85, 1305.42$ and 1336.60 Å. The redshift was determined by calculating the cross-correlation function between region 9300-10200Å of the quasar spectrum and the redshifted composite SDSS quasar spectrum³⁸. The fitted wavelength range did not include the Ly α line. The best correlation with a correlation coefficient of 0.86 was achieved for a redshift of $z = 6.618 \pm 0.02$.

The near-zone size. To measure the size of the ionized HII region around the quasar, we first smoothed the quasar spectrum to a resolution of 20Å. The transmission in the near zone was calculated by dividing the smoothed spectrum by power-law continuum $F_{\lambda} \sim \lambda^{-1.1}$, and the Lorentzian and Gaussian fitted to the Ly α and NV lines. When measuring the near zone, we corrected the quasar redshift for a systematic offset of about +0.02. This systematic offset was reported between the MgII redshift and redshifts derived from high-ionization lines³⁹. We measured a proper near zone of 3 ± 1 Mpc as a region where the transmitted flux drops below 10% of extrapolated continuum emission⁴⁰. The size of the near zone scaled to $M_{1450} = -27$ is 4 ± 1 Mpc³¹.

References

1. Becker, R. H. *et al.* Evidence for Reionization at $z \sim 6$: Detection of a Gunn-Peterson Trough in a $z=6.28$ Quasar. *Astron. J.*, **122**, 2850-2857 (2001)
2. Mortlock, D. J. *et al.* A luminous quasar at a redshift of $z = 7.085$. *Nature*, **474**, 616-619 (2011)
3. Venemans, B. P. *et al.* Discovery of Three $z > 6.5$ Quasars in the VISTA Kilo-Degree Infrared Galaxy (VIKING) Survey. *Astrophys. J.*, **779**, 24-37 (2013)
4. Venemans, B.P. *et al.* The Identification of Z-dropouts in Pan-STARRS1: Three Quasars at $6.5 < z < 6.7$. *Astrophys. J. Lett.*, **801**, L11-L18 (2015)
5. Kaiser, N. *et al.* The Pan-STARRS wide-field optical/NIR imaging survey. *Proc. SPIE*, **7733**, 14 (2010)
6. Schlafly, E. F. *et al.* Photometric Calibration of the First 1.5 Years of the Pan-STARRS1 Survey. *Astrophys. J.*, **756**, 158 (14pp) (2012)
7. Wu, X. B. *et al.* An ultraluminous quasar with a twelve-billion-solar-mass black hole at redshift 6.30. *Nature*, **518**, 512-515 (2015)
8. De Rosa, G. *et al.* Black Hole Mass Estimates and Emission-line Properties of a Sample of Redshift $z > 6.5$ Quasars. *Astrophys. J.*, **790**, 145-159 (2014)
9. Bañados, E. *et al.* The Pan-STARRS1 distant $z > 5.6$ quasar survey: more than 100 quasars within the first Gyr of the universe. arXiv.org e-Print archive <https://arxiv.org/abs/1608.03279> (2016)
10. Puchnarewicz, E. M., Mason, K. O. & Siemiginowska, A. The UV spectrum of the narrow-line Seyfert 1 galaxy, RE J1034+396. *MNRAS*, **293**, L52-L56 (1998)
11. Mathur, S. Narrow-line Seyfert 1 galaxies and the evolution of galaxies and active galaxies. *MNRAS*, **314**, L17-L20 (2000)
12. Boroson, T. A. Black Hole Mass and Eddington Ratio as Drivers for the Observable Properties of Radio-loud and Radio-quiet QSOs. *Astrophys. J.*, **565**, 78-85 (2002)
13. Bian, W. & Zhao, Y. Black hole masses in narrow-line Seyfert 1 galaxies. *MNRAS*, **352**, 823-827 (2004)
14. Richards, G. T. *et al.* Spectral Energy Distributions and Multiwavelength Selection of Type 1 Quasars. *Astrophys. J. Suppl.*, **166**, 470-497 (2006)
15. Willott, C. J. *et al.* Eddington-limited Accretion and the Black Hole Mass Function at Redshift 6. *Astrophys. J.*, **140**, 546-560 (2010)

16. Peterson, B. M. & Wandel, A. Keplerian Motion of Broad-Line Region Gas as Evidence for Supermassive Black Holes in Active Galactic Nuclei. *Astrophys. J.*, **521**, L95-L98 (1999)
17. Hu, E.M. *et al.* An Ultraluminous Ly α Emitter with a Blue Wing at $z = 6.6$. *Astrophys. J. Lett.*, **825**, 825-829 (2016)
18. Ivezić, Ž. *et al.* Quasar variability measurements with SDSS repeated imaging and POSS data. In *IAU Symp. 222, The Interplay Among Black Holes, Stars and ISM in Galactic Nuclei*, (eds. Storchi-Bergmann, T., Ho, L. C. & Schmitt H. R.) p.525 (Cambridge: Cambridge Univ. Press, 2004)
19. MacLeod, C. L. *et al.* A Description of Quasar Variability Measured Using Repeated SDSS and POSS Imaging. *Astrophys. J.*, **753**, 106 (21pp) (2012)
20. Turner, T. J. *et al.* Multiwavelength Monitoring of the Narrow-Line Seyfert 1 Galaxy Arakelian 564. I. ASCA Observations and the Variability of the X-Ray Spectral Components. *Astrophys. J.*, **561**, 131-145 (2001)
21. Romano, P., Turner, T. J., Mathur, S., & George I. M. A 12 Day ASCA Observation of the Narrow-Line Seyfert 1 Galaxy Ton S180: Time-selected Spectroscopy. *Astrophys. J.*, **564**, 162-175 (2002)
22. Peterson, B. M. *An Introduction to Active Galactic Nuclei*. p.82 (Cambridge: Cambridge Univ. Press, 1997)
23. Peterson, B.M. & Wandel, A. Evidence for Supermassive Black Holes in Active Galactic Nuclei from Emission-Line Reverberation. *Astrophys. J.*, **540**, L13-L16 (2000)
24. Collier, S. *et al.* Multiwavelength Monitoring of the Narrow-Line Seyfert 1 Galaxy Arakelian 564. II. Ultraviolet Continuum and Emission-Line Variability. *Astrophys. J.*, **561**, 146-161 (2001)
25. Chambers, K. PS1 and the PS1 science mission. *Proc. Advanced Maui Optical and Space Surveillance Technologies Conference*, (ed. Ryan, S.) p. E39 (Kihei, HI: The Maui Economic Development Board, 2006)
26. Gaskell, C. M. & Klimek, E. S. Variability of Active Galactic Nuclei from Optical to X-ray Regions. *Astron. Astrophys. Trans.*, **22**, 661-680 (2003)
27. Krolik, J.H. & Kallman, T.R. The effects of thermal accretion disk spectra on the emission lines from active galactic nuclei. *Astrophys. J.*, **324**, 714-720 (1988)
28. Green, P.J. The Relationship between the High-Energy Continuum and Emission Lines in Quasars: A Low-Redshift Sample. *Astrophys. J.*, **467**, 61-75 (1996)
29. Orsi, A. *et al.* The nebular emission of star-forming galaxies in a hierarchical universe. *MNRAS*, **443**, 799-814 (2014)

30. Hayes, M. *et al.* On the Redshift Evolution of the Ly α Escape Fraction and the Dust Content of Galaxies. *Astrophys. J.*, **730**, 8 (13pp) (2011)
31. Carilli, C. L. *et al.* Ionization Near Zones Associated with Quasars at $z \sim 6$. *Astrophys. J.*, **714**, 834-839 (2010)
32. Grier, C. J. *et al.* A Reverberation Lag for the High-ionization Component of the Broad-line Region in the Narrow-line Seyfert 1 Mrk 335. *Astrophys. J.*, **744**, L4 (5pp) (2012)
33. Rafter, S. E. *et al.* Reverberation Mapping of a Low-mass Black Hole in a Narrow-line Seyfert 1 Galaxy. *Astrophys. J.*, **773**, 24 (7pp) (2013)
34. Kaspi, S. *et al.* Reverberation Measurements for 17 Quasars and the Size-Mass-Luminosity Relations in Active Galactic Nuclei. *Astrophys. J.*, **533**, 631-649 (2000)
35. Peterson, B. M. *et al.* Central Masses and Broad-Line Region Sizes of Active Galactic Nuclei. II. A Homogeneous Analysis of a Large Reverberation-Mapping Database. *Astrophys. J.*, **613**, 682-699 (2004)
36. Wright, E. L. *et al.* The Wide-field Infrared Survey Explorer (WISE): Mission Description and Initial On-orbit Performance. *Astrophys. J.*, **140**, 1868-1881 (2010)
37. Kashikawa, N. *et al.* FOCAS: The Faint Object Camera and Spectrograph for the Subaru Telescope. *Publ. of the Astron. Soc. of Japan*, **54**, 819-832 (2002)
38. Vanden Berk, D. E. *et al.* Composite Quasar Spectra from the Sloan Digital Sky Survey. *Astrophys. J.*, **122**, 549-564 (2001)
39. Richards, G. T. *et al.* Broad Emission-Line Shifts in Quasars: An Orientation Measure for Radio-Quiet Quasars? *Astron. J.*, **124**, 1-17 (2002)
40. Fan, X. *et al.* Constraining the Evolution of the Ionizing Background and the Epoch of Reionization with $z \sim 6$ Quasars. II. A Sample of 19 Quasars. *Astron. J.*, **132**, 117-136 (2006)
41. Woo, S. C., Turnshek, D. A., Badenes, C., & Bickerton, S. Variability of broad emission lines in high-luminosity, high-redshift quasars. *MNRAS*, **434**, 1411-1421 (2013)

Acknowledgements

The research project was supported by the Ministry of Science and Technology of Taiwan, grant No. MOST 103-2119-M-008-017-MY3 and MOST 105-2811-M-008-074. The Pan-STARRS1 Surveys have been made possible through contributions of the Institute for Astronomy, University of Hawaii, the Pan-STARRS Project Office, the

Max-Planck Society and its participating institutes, Max-Planck-Institute for Astronomy, Heidelberg and Max-Planck-Institute for Extraterrestrial Physics, Garching, The Johns Hopkins University, Durham University, University of Edinburgh, Queens University Belfast, Harvard-Smithsonian Center for Astrophysics, the Las Cumbres Observatory Global Telescope Network Incorporated, the National Central University of Taiwan, the Space Telescope Science Institute, the National Aeronautics and Space Administration under grant No. NNX08AR22G issued through the Planetary Science Division of the NASA Science Mission Directorate, the National Science Foundation under grant AST-1238877, the University of Maryland, and Eotvos Lorand University (ELTE). This research has made use of the services of the ESO Science Archive Facility.

Author contributions statement

E.K. selected the source, observed and analysed the data. C.-Y. H. supervised the data interpretation and edited the manuscript. P.-C. Y. contributed to the calculations and edited the manuscript. W.-P. C. and J.-K.G. gave data support for conducting the source selection. All authors discussed the results and implications and commented on the manuscript at all stages.

Additional information

Competing financial interests The authors declare that they have no competing financial interests.

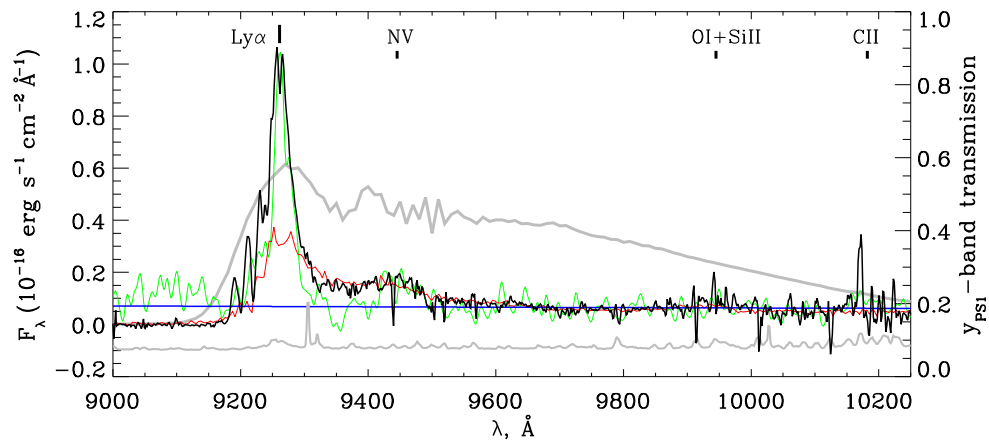


Figure 1. FOCAS spectrum of PSO J006.1240+39.2219 (black line). The displayed spectrum is smoothed with the Gaussian filter using a smoothing window of 5\AA . The sigma spectrum shown with a grey line is offset for better representation. The $\text{Ly}\alpha$ line is detected with a signal-to-noise ratio (SNR) of 34. The SNR ratios of the spectrum at the positions of the NV, OI+SiII and CII emission lines are 15, 4 and 1. The widths of the $\text{Ly}\alpha$ line, deblended and fitted with the Lorentzian profile, is estimated to be 1300 km s^{-1} . The composite spectrum of $z > 5.6$ quasars with strong $\text{Ly}\alpha$ emission⁹ is overplotted in red. The redshifted UV spectrum of the NLS1 galaxy RE J1034+396 at $z=0.043$ is shown in green. (The spectra are scaled to the NV emission line of PSO J006.1240+39.2219). The power-law continuum fit over spectral windows 9550 - 9900 and 10000 - 10150 \AA ($F_\lambda \sim \lambda^{-1.1}$) is shown with a blue line. The transmission curve of the PS1 y-band filter is plotted with a thick grey line.

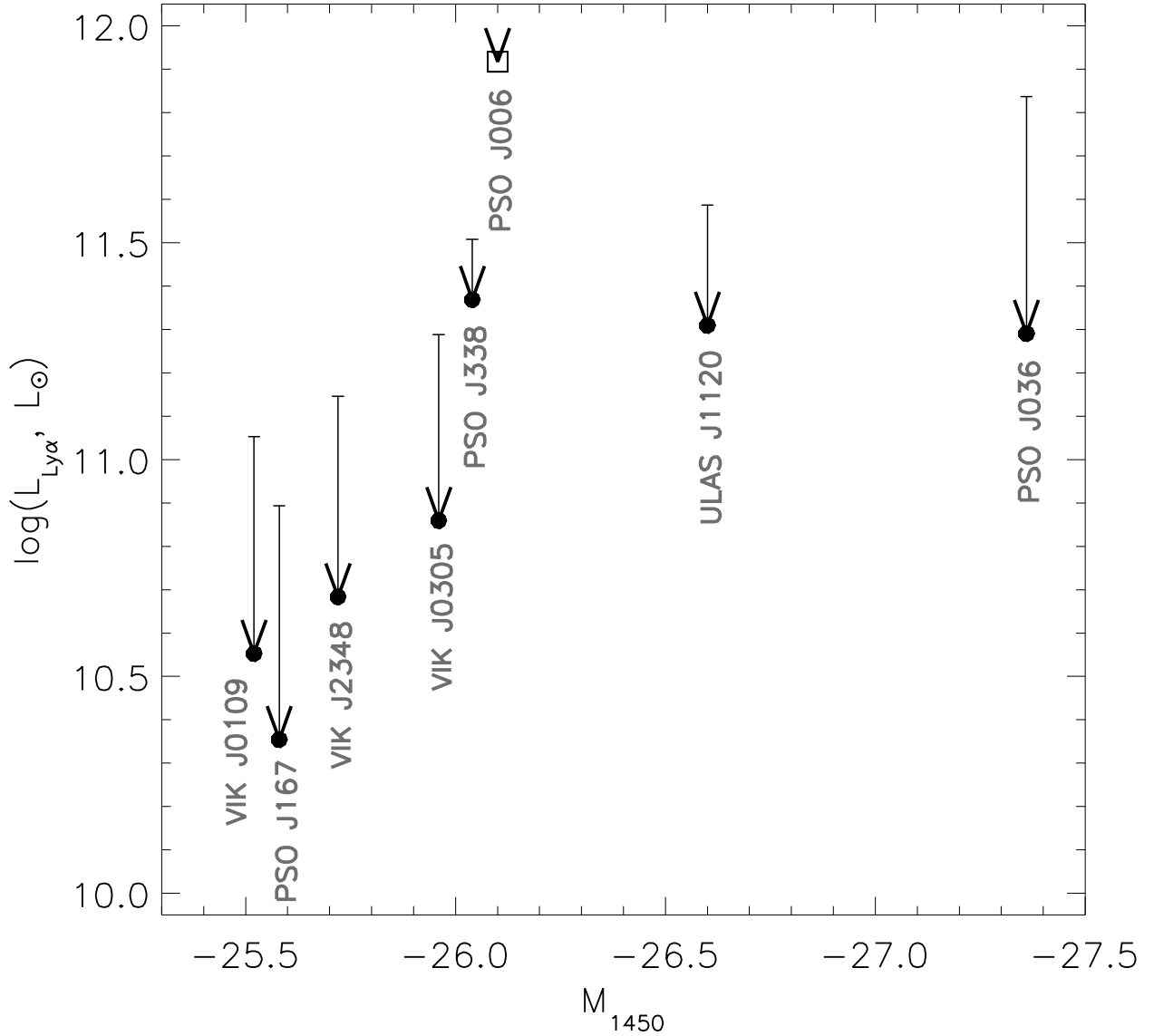


Figure 2. Absolute UV magnitude M_{1450} of quasars at redshift $z > 6.5$ versus $\text{Ly}\alpha$ line luminosity. The quasars ULAS J1120+0641², VIK J0109-3047³, VIK J2348-3054³, VIK J0305-3150³, PSO J167-13⁴, PSO J338+29⁴, PSO J036+03⁴ are marked with black circles, PSO J006.1240+39.2219 is shown with an open square. The $\text{Ly}\alpha$ line luminosity is estimated by integrating the line flux between 1204–1229Å ($\sim 6170 \text{ km s}^{-1}$)⁴¹. The upper limits correspond to the luminosity of the $\text{Ly}\alpha$ line obtained without continuum subtraction from the line flux. The continuum contribution into the $\text{Ly}\alpha$ line of PSO J006.1240+39.2219 is estimated to be less than 10% (within the region marked by the square) and is significantly less than in the other $z > 6.5$ quasars.

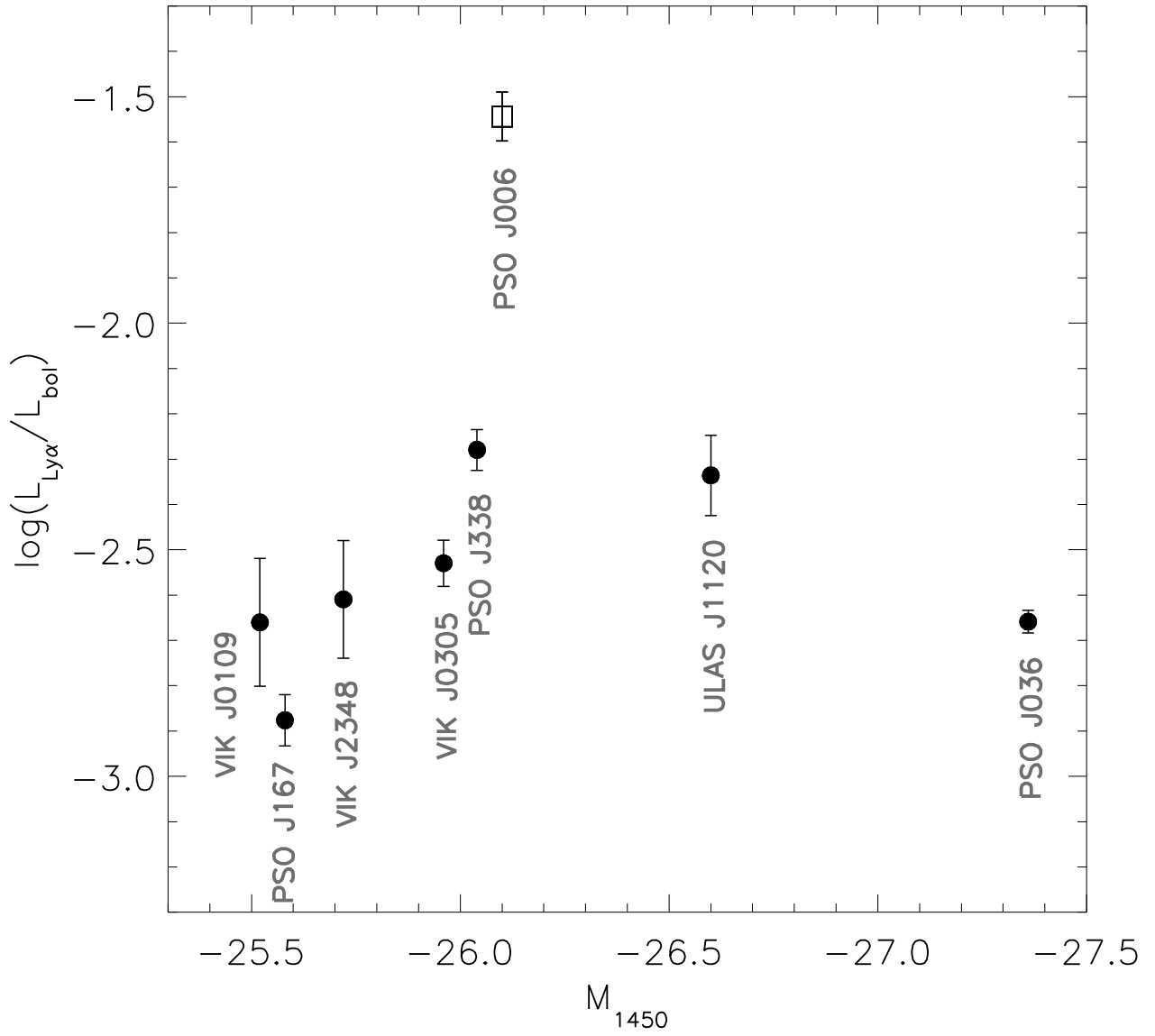


Figure 3. Absolute UV magnitude M_{1450} of quasars at redshift $z > 6.5$ versus $\text{Ly}\alpha$ line luminosity expressed as a fraction of the bolometric luminosity. The object notation is similar to the previous figure.

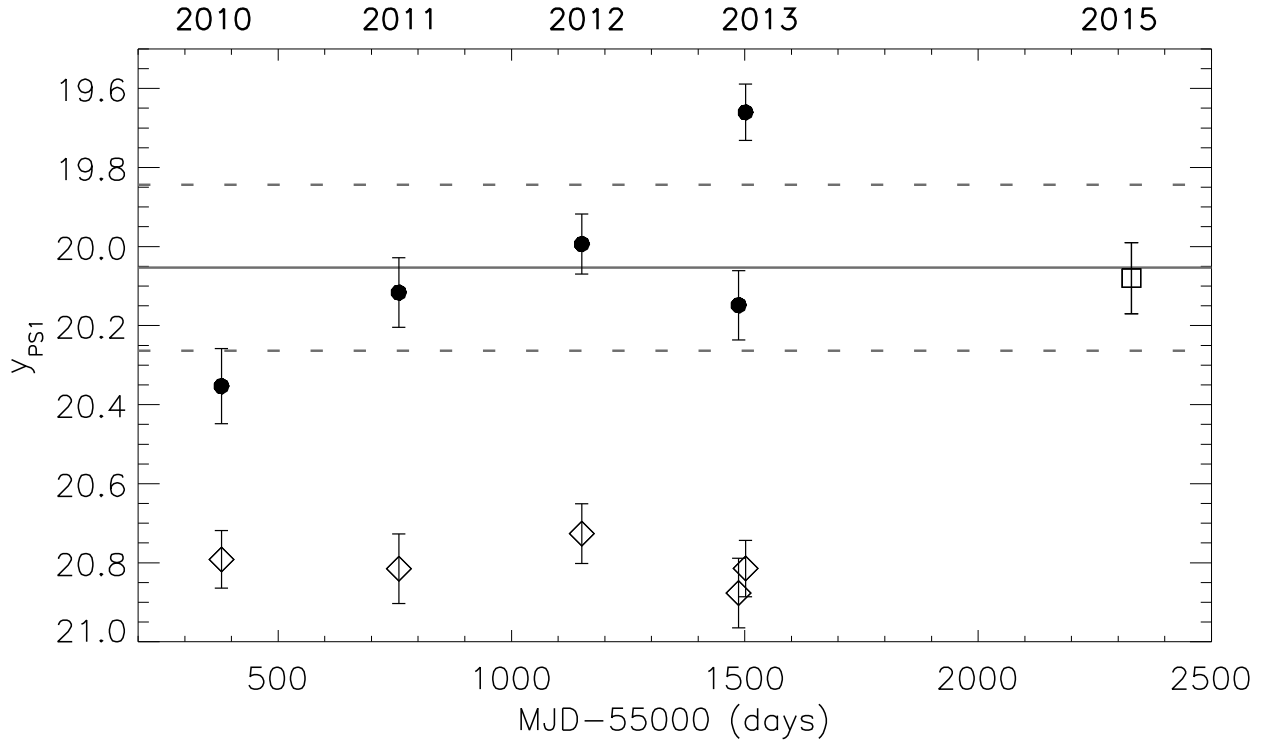


Figure 4. The y_{PS1} -band light curve of PSO J006.1240+39.2219. Black points show the quasar brightness measured using aperture photometry of the PS1 images taken between June 2010 and July 2013. At each of the epochs, the quasar was observed at least two times for a total of 60s. The measured quasar flux and uncertainty at the different epochs are estimated as the mean and standard deviation of five independent quasar flux measurements relative to five nearby faint stars of $\sim 19.5\text{--}20.0$ mag. The solid and dotted grey lines correspond to a multi-epoch mean and its $\pm 2.5\sigma$ error of 20.05 ± 0.21 mag. In 2010 the quasar was fainter of its mean brightness by 0.24 mag. Within 15 days in 2013, it became brighter than its mean brightness by ~ 0.4 mag (which is 4.6σ off the multi-epoch mean), showing short-term variability. The overall brightness change between 2010 and 2013 is ~ 0.7 mag. The open square shows the brightness of the quasar in 2015 estimated from its discovery spectrum by integrating the flux through the y_{PS1} passband. The light curve of one of the nearby faint stars of 19.65 ± 0.07 mag chosen for quasar flux calibration, is shown with diamonds. (For better representation the light curve of the star is shifted by +1.15 mag.)